entropy

MDPI

Article

Isospectral Twirling and Quantum Chaos

Lorenzo Leone *, Salvatore F. E. Oliviero and Alioscia Hamma

Physics Department, University of Massachusetts Boston, Boston, MA 02125, USA; S.Oliviero001@umb.edu (S.F.E.O.); alioscia.hamma@umb.edu (A.H.)

* Correspondence: Lorenzo.Leone001@umb.edu

Abstract: We show that the most important measures of quantum chaos, such as frame potentials, scrambling, Loschmidt echo and out-of-time-order correlators (OTOCs), can be described by the unified framework of the isospectral twirling, namely the Haar average of a k-fold unitary channel. We show that such measures can then always be cast in the form of an expectation value of the isospectral twirling. In literature, quantum chaos is investigated sometimes through the spectrum and some other times through the eigenvectors of the Hamiltonian generating the dynamics. We show that thanks to this technique, we can interpolate smoothly between integrable Hamiltonians and quantum chaotic Hamiltonians. The isospectral twirling of Hamiltonians with eigenvector stabilizer states does not possess chaotic features, unlike those Hamiltonians whose eigenvectors are taken from the Haar measure. As an example, OTOCs obtained with Clifford resources decay to higher values compared with universal resources. By doping Hamiltonians with non-Clifford resources, we show a crossover in the OTOC behavior between a class of integrable models and quantum chaos. Moreover, exploiting random matrix theory, we show that these measures of quantum chaos clearly distinguish the finite time behavior of probes to quantum chaos corresponding to chaotic spectra given by the Gaussian Unitary Ensemble (GUE) from the integrable spectra given by Poisson distribution and the Gaussian Diagonal Ensemble (GDE).

Keywords: quantum chaos; information scrambling; entanglement; twirling

Citation: Leone, L.; Oliviero, S.F.E.; Hamma, A. Isospectral Twirling and Quantum Chaos. *Entropy* **2021**, *23*, 1073. https://doi.org/10.3390/e23081073

Academic Editors: Levan Chotorlishvili and Arthur Ernst

Received: 26 July 2021
Accepted: 16 August 2021
Published: 19 August 2021

1. Introduction

The onset of chaotic dynamics is at the center of many important phenomena in quantum many-body systems, from thermalization in a closed system [1–11] to scrambling of information in quantum channels [12–17], black hole dynamics [18–21], entanglement complexity [22,23], to pseudorandomness in quantum circuits [24–28], and finally, the complexity of quantum evolutions [29–32]. Several probes of quantum chaos have been studied in recent years [33–36]. Chaos, equilibration, thermalization and other related phenomena are described by the behavior of entanglement growth and typicality, the Loschmidt echo, and out-of-time-order correlation functions (OTOCs) [20,37–45]. Information scrambling is characterized by tripartite mutual information [12,13] and its connection OTOCs. Pseudorandomness is characterized by the frame potential, which describes the adherence to moments of the Haar measure [46,47]; the complexity of entanglement is characterized by the adherence to the random matrix theory distribution of the gaps in the entanglement spectrum [22,23].

Random matrix theory (RMT) has been extensively studied and applied to quantum chaos [48–53]. The quantization of classical chaotic systems has often resulted in quantum Hamiltonians with the same level of spacing statistics of a random matrix taken from the Gaussian Unitary Ensemble (GUE). One could take the behavior of OTOCs, entanglement, frame potentials and other probes under a time evolution induced by a chaotic Hamiltonian, e.g., a random Hamiltonian from GUE, and define it as the characteristic behavior of these quantities for quantum chaos [54–56]. Though we agree with the heuristics of this approach, it would be important to compare the time behavior of these probes in

systems that are not characterized by a spectrum given by a random matrix, or on the other hand, by Hamiltonians whose eigenvectors are not a random basis according to the Haar measure, e.g., Hamiltonians with eigenvectors that, although possessing high entanglement, do not contain any magic, that is, they are stabilizer states. Attempts at showing the difference in behavior between chaotic and non-chaotic behavior are often limited to specific examples [38,57]. Moreover, given the proliferation of probes to quantum chaos, one does feel the necessity of having a unified framework to gather together all these results.

In this paper, we set out to provide such a unifying framework and to prove that one can clearly distinguish chaotic from non-chaotic dynamics. The framework is provided by the *isospectral twirling* $\hat{\mathcal{R}}^{(2k)}(U)$, that is, the Haar average of a $k-$fold channel. This operation randomizes over the eigenstates of a unitary channel U but leaves the spectrum invariant. In this way, one obtains quantities that are functions of the spectrum only. The unitary channel represents the quantum evolution induced by a Hamiltonian. Chaotic Hamiltonians feature spectra obeying the random matrix theory, e.g., GUE, while integrable systems possess spectra obeying other statistics [58–61]. The main results of this paper are: (i) the isospectral twirling unifies all the fundamental probes $\mathcal{P}$ used to describe quantum chaos in the form of $\langle \mathcal{P}_{\mathcal{O}} \rangle_G = \mathrm{tr}[\tilde{T}\mathcal{O}\hat{\mathcal{R}}^{(2k)}]$, where $\tilde{T}$ is a rescaled permutation operator, $\mathcal{O}$ characterizes the probe, $\langle \cdot \rangle_G$ is the Haar average and (ii) by considering the isospectral twirling associated to a $k-$doped Clifford group $\mathcal{C}(d)$, we show that the asymptotic temporal behavior of the OTOCs interpolates between a class of integrable models and quantum chaos and does not depend on the specific spectrum of the Hamiltonian; (iii) finally, by computing the isospectral twirling for the spectra corresponding to the chaotic Hamiltonians in GUE and integrable ones—Poisson, Gaussian Diagonal Ensemble (GDE)—the isospectral twirling can distinguish chaotic from non-chaotic behavior in the temporal profile of the probes, though all the spectra lead to the same asymptotic behavior—a sign of the fact that chaos is not solely determined by the spectrum of the Hamiltonian but also by its eigenvectors.

2. Isospectral Twirling

Let $\mathcal{H} \simeq \mathbb{C}^d$ be a $d-$dimensional Hilbert space and let $U \in \mathcal{U}(\mathcal{H})$ with spectral resolution $U = \sum_k e^{-iE_k t}\Pi_k$, where Π_k are orthogonal projectors on $\mathcal{H}$. We can think of the $\mathrm{Sp}(H) \equiv \{E_k\}_{k=1}^d$ as the spectrum of a Hamiltonian H. Through H we can generate an isospectral family of unitaries $\mathcal{E}_H \equiv \{U_G(H)\}_G := \{G^\dagger \exp\{-iHt\}G,\ G \in \mathcal{U}(\mathcal{H})\}$. Define *isospectral twirling* as the $2k-$fold Haar channel of the operator $U^{\otimes k,k} \equiv U^{\otimes k} \otimes U^{\dagger \otimes k}$ by

$$\hat{\mathcal{R}}^{(2k)}(U) := \int dG\, G^{\dagger \otimes 2k}\left(U^{\otimes k,k}\right) G^{\otimes 2k} \tag{1}$$

where dG represents the Haar measure over $\mathcal{U}(\mathcal{H})$. This object has been previously used to demonstrate convergence to equilibrium under a random Hamiltonian [62] or the behavior of random quantum batteries [63]. Under the action of (1), the spectrum of U is preserved. A general way to compute the above average is to use the Weingarten functions [64]. We obtain:

$$\hat{\mathcal{R}}^{(2k)}(U) = \sum_{\pi\sigma} (\tilde{\Omega}^{-1})_{\pi\sigma} \mathrm{tr}(\tilde{T}_\pi^{(2k)} U^{\otimes k,k}) \tilde{T}_\sigma^{(2k)} \tag{2}$$

where $\tilde{T}_\pi^{(2k)} \equiv T_\pi^{(2k)}/d_\pi^{(2k)}$, $\pi, \sigma \in S_{2k}$ are (rescaled) permutation operators of order $2k$, $d_\pi^{(2k)} = \mathrm{tr} T_\pi^{(2k)}$ and $(\tilde{\Omega}^{-1})_{\pi\sigma} \equiv [\mathrm{tr}(\tilde{T}_\pi^{(2k)} \tilde{T}_\sigma^{(2k)})]^{-1}$ are rescaled Weingarten functions. Notice that, through U, the isospectral twirling is a function of the time t.

3. The Integrability-Chaos Transition

The Hamiltonian generating the unitary temporal evolution in a closed quantum system can be written in its spectral resolution $H = \sum_i E_i \Pi_i$, showing explicitly that

the dynamics are contained both in the eigenvalues and the eigenvectors of H. We now show that information about the asymptotic temporal behavior is contained in the way we pick the eigenvectors of H. To this end, consider a system of N qubits, $\mathcal{H} = \mathbb{C}^{2^N}$, and a Hamiltonian diagonal in the computational basis $\{|i\rangle\}_{i=1}^{2^N}$, namely $H = \sum_i E_i \Pi_i$ with $\Pi_i = |i\rangle\langle i|$ orthogonal projectors. Define then the average asymptotic unitary

$$U_\infty^{\otimes 2,2} := \lim_{t\to\infty} \overline{U^{\otimes 2,2}}^{P(E_i)} \tag{3}$$

where the average is taken over a Schwartzian probability distribution of spectra. The isospectral twirling of $U_\infty^{\otimes 2,2}$ thus does not depend on the distribution of the eigenvalues $P(E_i)$.

We now map these projectors by $\Pi_i \mapsto C\Pi_i C^\dagger$ with $C \in \mathcal{C}(d)$ the Clifford group. These projectors are not typical in the Hilbert space and they cannot be clearly associated with chaotic behavior, for instance, it is not clear whether they feature ETH. They would possess typical entanglement, but its fluctuations obtained by the Haar measure on the unitary group are not the same. Define the $Cl-$Isospectral twirling for $U_\infty^{\otimes 2,2}$ as

$$\mathcal{R}_{Cl}^{(4)}(U_\infty) := \int_{\mathcal{C}(2^N)} \mathrm{d}C C^{\dagger\otimes 4} U_\infty^{\otimes 2,2} C^{\otimes 4} \tag{4}$$

A general way to compute the Clifford average of order four is to use the generalized Weingarten functions formula, which is a rearrangement of the formula shown in [65]:

$$\begin{aligned}\mathcal{R}_{Cl}^{(4)}(U_\infty) = &\sum_{\pi\sigma} W_g^+(\pi\sigma)\mathrm{tr}(U_\infty^{\otimes 2,2} Q T_\sigma) Q T_\pi \\ &+ W_g^-(\pi\sigma)\mathrm{tr}(U_\infty^{\otimes 2,2} Q^\perp T_\sigma) Q^\perp T_\pi\end{aligned} \tag{5}$$

where $Q = \frac{1}{d^2}\sum_{P\in\mathcal{P}(2^N)} P^{\otimes 4}$, $Q^\perp = \mathbb{1}^{\otimes 4} - Q$ and $P \in \mathcal{P}(2^N)$ elements of the Pauli group on N-qubits, while

$$W_g^\pm(\pi\sigma) := \sum_{\lambda \,|\, D_\lambda^\pm \neq 0} \frac{d_\lambda^2}{(4!)^2} \frac{\chi^\lambda(\pi\sigma)}{D_\lambda^\pm} \tag{6}$$

here λ labels the irreducible representations of the symmetric group S_4, $\chi^\lambda(\pi\sigma)$ are the characters of S_4 depending on the irreducible representations λ, d_λ is the dimension of the irreducible representations λ, $D_\lambda^+ = \mathrm{tr}(QP_\lambda)$ and $D_\lambda^- = \mathrm{tr}(Q^\perp P_\lambda)$ where P_λ are the projectors onto the irreducible representations of S_4, and finally, T_σ are permutation operators corresponding to the permutation $\sigma \in S_4$.

Let the unitary evolution be generated by a $l-$doped Hamiltonian $H_l = C^{(l)\dagger} H_0 C^{(l)}$ where

$$C^{(l)} = \prod_r C_r^\dagger K_r \tag{7}$$

In the equation above, every $C_r \in \mathcal{C}(d)$ is an element of the Clifford group, while K_r is a single qubit gate not belonging to the Clifford group. In this way, we have doped the Clifford Hamiltonian with non-Clifford resources. Notice that, for $l = 0$, the Hamiltonian is the sum of commuting Pauli strings, and it is therefore integrable. We want to show that by inserting the gates K_r, we obtain a transition to quantum chaotic behavior. This result would also show that integrability can be deformed in a "smooth" way and attain a crossover to quantum chaos. To this end, we use a particular probe to quantum chaos given by the OTOCs, as we shall see in the next section.

4. OTOCs

Scrambling of information can be measured by two quantities, the OTOCs [33] and the tripartite mutual information (TMI) [13]; namely, the decay of the OTOC implies the decay of the TMI [12,13]. In this section, we show how the OTOCs are described by the isospectral

twirling. Consider $2k$ local, non-overlapping operators A_r, B_r, $r \in [1,k]$. The infinite temperature $4k-$point OTOC is defined as

$$\begin{aligned} \mathrm{OTOC}_{4k}(t) &= d^{-1}\mathrm{tr}(A_1^\dagger(t)B_1^\dagger\cdots A_k^\dagger(t)B_k^\dagger \\ &\times A_1(t)B_1\cdots A_k(t)B_k) \end{aligned} \tag{8}$$

where $A_l(t) = e^{iHt}A_l e^{-iHt}$. Define $\mathcal{A}_l := A_l^\dagger \otimes A_l$ and similarly for $\mathcal{B}$.

Proposition 1. *The isospectral twirling of the $4k-$point OTOC is given by*

$$\langle OTOC_{4k}(t)\rangle_G = \mathrm{tr}(\tilde{T}_\pi^{(4k)}(\otimes_{l=1}^k \mathcal{A}_l \otimes_{l=1}^k \mathcal{B}_l)\hat{\mathcal{R}}^{(4k)}(U)) \tag{9}$$

See Appendix A for the proof. For $k = 1$, we obtain the 4-point OTOC, see Appendix A.2:

$$\langle \mathrm{OTOC}_4(t)\rangle_G = \mathrm{tr}(\tilde{T}_{(1423)}(\mathcal{A}\otimes\mathcal{B})\hat{\mathcal{R}}^{(4)}(U)) \tag{10}$$

With the above formula, we compute the asymptotic value of the $4-$point OTOC:

$$\begin{aligned} \langle \mathrm{OTOC}_4\rangle_{Cl}(\infty) =& \sum_{\pi\sigma} W_g^+(\pi\sigma)\mathrm{tr}(U_\infty^{\otimes 2,2} Q T_\sigma) \\ &\times \mathrm{tr}(\tilde{T}_{(1423)}(\mathcal{A}\otimes\mathcal{B})Q T_\pi) \\ &+ W_g^-(\pi\sigma)\mathrm{tr}(U_\infty^{\otimes 2,2} Q^\perp T_\sigma) \\ &\times \mathrm{tr}(\tilde{T}_{(1423)}(\mathcal{A}\otimes\mathcal{B})Q^\perp T_\pi) \end{aligned} \tag{11}$$

Proposition 2. *By setting in (10) $\mathcal{A}$ and $\mathcal{B}$ as non-overlapping Pauli operators on qubits, the asymptotic value of the $Cl-$Isospectral twirling of the $4-$point OTOC reads*

$$\langle OTOC_4\rangle_{Cl}(\infty) = \frac{2}{(d+2)} \tag{12}$$

See Appendix B for the proof. This value has to be compared with the asymptotic value for the isospectral twirling obtained by averaging the full unitary group:

$$\langle \mathrm{OTOC}_4\rangle_G(\infty) = \frac{1}{(d+1)(d+3)} \tag{13}$$

showing a clear separation in the asymptotic decay of the OTOCs between the full Unitary and Clifford cases. For example, this shows that one cannot obtain the same asymptotic behavior by using only Clifford resources in a random quantum circuit.

Now we consider $l-$doped Hamiltonians by doping with $T-$gates, without loss of generality. Using the technique in [66], a lengthy but straightforward calculation gives the following theorem.

Theorem 1. *The asymptotic value of the averaged $4-$point OTOC for an $l-$doped Hamiltonian reads:*

$$\lim_{t\to\infty} \overline{\langle OTOC_4(t)\rangle_{\mathcal{C}_l}}^{P(E_i)} = \left(\frac{3}{4}\right)^l \frac{2}{d} + \frac{1}{d^2} + \Omega(d^{-3}) \tag{14}$$

As we can see, this result interpolates between the Clifford and Haar cases of Equations (12) and (13).

The above equation shows a crossover between integrable and quantum chaotic behavior. The first term shows the integrable scaling of the OTOCs, while the second term shows the universal Haar chaotic behavior, see Proposition 2 above. The integrable term is exponentially suppressed in the doping parameter l. As a corollary, we obtain that iff $l = \Omega(n)$, $l-$doped stabilizer Hamiltonians attain the same scaling of *Haar* Hamiltonians for the infinite time $4-$OTOCs.

5. Finite Time Behavior

From now on, we are concerned with finite-time behavior. Such behavior is ruled by spectral properties, while the eigenvectors are being chosen to be Haar-like, that is, we use the Haar-isospectral twirling (1). We will see that, insofar only the properties of the spectrum of the Hamiltonian H are concerned, different ensembles of spectra associated with different RMT distinguish the temporal profile of the chaos probes in the transient before the onset of the asymptotic behavior, which is the same for all the ensembles of spectra with a Schwartzian probability distribution [67]. By averaging over the unitary group in Equation (1), we have, on the one hand, effectively erased any information coming from the eigenstates of the Hamiltonian, and on the other hand, already introduced some of the properties of chaotic or ergodic Hamiltonians. For instance, these eigenvectors typically obey the eigenstate thermalization hypothesis [1,2,4,68]. In fact, it is striking that the spectra should have any effect at all once we use random eigenvectors. In order to examine the spectral properties revealed in the finite time behavior, we need to consider the spectral form factors.

Taking the trace of Equation (1), one obtains the $2k-$point spectral form factors: $\mathrm{tr}(\hat{\mathcal{R}}^{(2k)}(U)) = |\mathrm{tr}(U)|^{2k} = (d + Q(t))^k$, which follows easily from the cyclic property of the trace and the fact that $\int dG = 1$. The object $Q(t) = \sum_{i \neq j} \cos[(E_i - E_j)t]$ [63] is related to the quantum advantage of the performance of random quantum batteries. For $k = 1, 2$ these spectral form factors read $|\mathrm{tr}(U)|^2 = \sum_{i,j} e^{i(E_i - E_j)t}$ and $|\mathrm{tr}(U)|^4 = \sum_{i,j,k,l} e^{i(E_i + E_j - E_k - E_l)t}$. More generally, consider the coefficients $\tilde{c}_\pi^{(2k)}(U) := \mathrm{tr}(\tilde{T}_\pi^{(2k)} U^{\otimes k,k})$. After the twirling, all the information about the spectrum of the Hamiltonian H is encoded in the $\tilde{c}_\pi^{(2k)}(U)$. We see that the $2k-$point spectral form factors come from the identity permutation $\pi = e$, such that $T_e^{(2k)} = \mathbb{1}^{\otimes 2k}$. For $k = 2$ and the permutation $T_\pi^{(4)} = T_{(12)(3)(4)}^{(4)} \equiv T_{(12)}^{(4)}$, we instead obtain another spectral form factor, namely $\tilde{c}_{(12)}^{(4)}(U) = d^{-3}\mathrm{tr}(U^2)\mathrm{tr}(U^\dagger)^2 = d^{-3}\sum_{i,j,k} e^{i(2E_i - E_j - E_k)t}$, which we will be needing later. Spectral form factors only depend on the spectrum of U. In particular, those we listed only depend on the gaps in the spectrum of H. For $k = 2$, we set up this lighter notation for objects that we will be frequently using: $\tilde{c}_e^{(2)} \equiv \tilde{c}_2$, $\tilde{c}_e^{(4)} \equiv \tilde{c}_4$, $\tilde{c}_{(12)}^{(4)} \equiv \tilde{c}_3$. From now on, we will omit the order of permutations T_π. The operators $\hat{\mathcal{R}}^{(2k)}(U)$ for $k = 1, 2$ are evaluated explicitly in [67].

In the following, we consider scalar functions $\mathcal{P}$ that depend on $U_G \equiv e^{-iG^\dagger H G t}$. The isospectral twirling of $\mathcal{P}$ is given by $\langle \mathcal{P}(t) \rangle_G = \int dG\, \mathcal{P}(G^\dagger U G)$. As we shall see, if $\mathcal{P}_\mathcal{O}$ is characterized by a bounded operator $\mathcal{O} \in \mathcal{B}(\mathcal{H}^{\otimes 2k})$, we obtain expressions of the form $\langle \mathcal{P}_\mathcal{O}(t) \rangle_G = \mathrm{tr}[\tilde{T}_\sigma \mathcal{O} \hat{\mathcal{R}}^{(2k)}(t)]$, where $\tilde{T}_\sigma$ is a normalized permutation operator, $\sigma \in S_{2k}$.

The average $\langle \mathcal{P}_\mathcal{O}(t) \rangle_G$ only depends on the spectrum of the generating Hamiltonian H. One can then average the value of $\langle \mathcal{P}_\mathcal{O}(t) \rangle_G$ over the spectra of an ensemble of Hamiltonians E. We denote such average as $\overline{\langle \mathcal{P}_\mathcal{O}(t) \rangle_G}^E$. One can observe that the average over the unitary group and average over the ensemble of Hamiltonians return a quantity that depends on the same eigenvector statistics but different eigenvalue statistics. In this procedure, we are neglecting the possible connection between the eigenvector statistics and the eigenvalue statistics, as suggested in the following papers [69,70]; this has been to highlight the role of how the spectrum is enough to distinguish the finite-time case. In the following, we are going to look at the following ensembles of Hamiltonians $E \equiv$ GUE, $E \equiv$ GDE or $E \equiv$ P, where the first is a class of chaotic Hamiltonians, and the others are classes of integrable Hamiltonians. It is important to remark that GUE is not the only a class of chaotic Hamiltonians; in random matrix theory, there are also two other classes of chaotic Hamiltonians: the Gaussian Orthogonal Ensemble (GOE) and the Gaussian Symplectic Ensemble (GSE) [50]. In the paper, we avoided considering these two classes of chaotic Hamiltonians since the behavior of the spectral coefficients $\overline{\tilde{c}_2(t)}^E$ and $\overline{\tilde{c}_4(t)}^E$ for GOE and GSE is not qualitatively different from the behavior of the coefficients for GUE [71]. Since the information about the spectrum of H is contained in the $\tilde{c}_\pi^{(2k)}(U)$,

computing $\overline{\langle \mathcal{P}_{\mathcal{O}}(t)\rangle_G}^E$ requires the knowledge of $\overline{\tilde{c}_\pi^{(2k)}(U)}^E$. The details of the random matrix calculations necessary to compute these quantities can be found in [67]. We present here in Figure 1 the temporal evolution of $\overline{\tilde{c}_4(t)}^E$, which is the most important factor for our goals. The 4−point spectral form factor $\tilde{c}_4$ is able to distinguish the chaotic (GUE) and the integrable (GDE, Poisson) regime via the system-size scaling d. Both GUE and Poisson reach the first minimum $\overline{\tilde{c}_4(t)}^E = O(d^{-2})$ in a time $t = O(1)$, while GDE reaches the asymptotic value $\lim_{t\to\infty} \overline{\tilde{c}_4(t)}^{\mathrm{GDE}} = d^{-3}(2d-1)$ in a time $t = O(\sqrt{\log d})$. We observe that GUE and Poisson present a quite different temporal profile: dropping below the asymptotic value, GUE reaches the dip $\overline{\tilde{c}_4(t)}^{\mathrm{GUE}} = O(d^{-3})$ in a time $t = O(d^{1/2})$ and then it rises to the asymptotic value $\lim_{t\to\infty} \overline{\tilde{c}_4(t)}^{\mathrm{GUE}} = d^{-3}(2d-1)$ in a time $O(d^{-1})$; on the other hand, Poisson never goes below $\lim_{t\to\infty} \overline{\tilde{c}_4(t)}^{\mathrm{P}} = d^{-3}(2d-1)$ reaching it in a time $O(d^{1/2})$.

In [54], the authors defined the twirling of the operator $U^{\otimes k,k}$, where $U \in \mathcal{E}_t^{\mathrm{GUE}} := \{e^{-iHt} \mid H \in \mathrm{GUE}\}$, i.e., $\Phi_{\mathcal{E}_t^{\mathrm{GUE}}}(U^{\otimes k,k}) = \int dH\, U^{\otimes k,k}$ with dH the unitarily invariant measure over the GUE ensemble of Hamiltonians. From $dH = d(W^\dagger H W)$, with $W \in \mathcal{U}(\mathcal{H})$, taking the Haar average over W, one easily obtains: $\Phi_{\mathcal{E}_t^{\mathrm{GUE}}}(U^{\otimes t,t}) = \int dH\, \hat{\mathcal{R}}^{(2k)}(U)$, i.e., the ensemble average of the isospectral twirling of Equation (1) over the GUE ensemble. This approach presents some limits of applicability; unlike the isospectral twirling, it only works for a unitarily invariant distribution of Hamiltonians. In particular, it would not allow us to distinguish GUE from the integrable distributions.

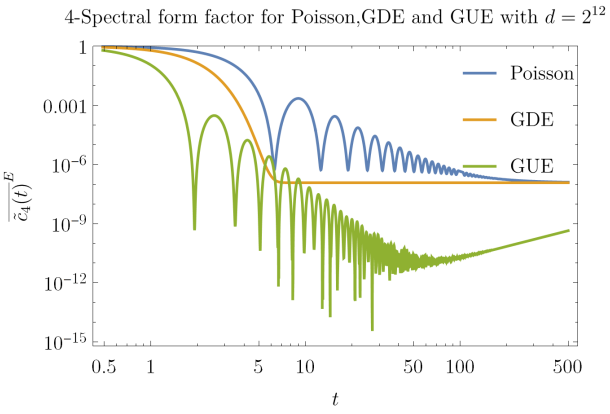

Figure 1. Log–log plot of the spectral form factor $\overline{\tilde{c}_4(t)}^E$ for different ensembles E ≡ P, E ≡ GDE and E ≡ GUE for $d = 2^{12}$. The starting value is 1, while the asymptotic value is $(2d-1)d^{-3}$.

We now apply the isospectral twirling to probe quantum chaos. Let us first study the finite time behavior of the OTOCs.

By setting in (10) $\mathcal{A}$ and $\mathcal{B}$ to be non-overlapping Pauli operators on qubits, one finds [67]:

$$\langle \mathrm{OTOC}_4(t)\rangle_G = \tilde{c}_4(t) - d^{-2} + O(d^{-4}) \tag{15}$$

As this result shows, the 4−point OTOCs distinguish chaotic from integrable behavior through the timescales dictated by $\tilde{c}_4$, see Figure 1. In a previous work [54], it was found $\langle \mathrm{OTOC}_4(t)\rangle_{\mathrm{GUE}} \simeq \tilde{c}_4(t)$; we instead remark the importance of the offset d^{-2}. Indeed, in [67], it is shown that after a time $O(d^{1/3})$ the 4−point spectral form factor: $\overline{\tilde{c}_4(t)}^{\mathrm{GUE}} = O(d^{-2})$, which makes the two terms in Equation (15) comparable.

6. Randomness of the Ensemble $\mathcal{E}_H$

A chaotic Hamiltonian should generate a random unitary according to the Haar measure. To this end, we ask how random the ensemble $\mathcal{E}_H$ generated by H is, i.e., how

much the unitaries $G^\dagger UG$ replicate the Haar distribution. We quantify randomness by computing the k-th frame potential of the ensemble $\mathcal{E}_H$ [46,47], defined as

$$\mathcal{F}^{(k)}_{\mathcal{E}_H} = \int dG_1 dG_2 \left| \mathrm{tr}\left(G_1^\dagger U^\dagger G_1 G_2^\dagger U G_2 \right) \right|^{2k}. \tag{16}$$

We have the following proposition:

Proposition 3. *The frame potential of $\mathcal{E}_H$ is the square Schatten $2-$norm of the isospectral twirling Equation (1):*

$$\mathcal{F}^{(k)}_{\mathcal{E}_H} = \|\hat{\mathcal{R}}^{(2k)}(U)\|_2^2 = \mathrm{tr}\left(\tilde{T}_{1\leftrightarrow 2} \left(\hat{\mathcal{R}}^{\dagger(2k)} \otimes \hat{\mathcal{R}}^{(2k)} \right) \right) \tag{17}$$

where $\tilde{T}_{1\leftrightarrow 2}$ is the swap operator between the first $2k$ copies of $\mathcal{H}$ and the second $2k$ copies.

See Appendix C.1 for the proof. The Haar value $\mathcal{F}^{(k)}_{\mathrm{Haar}} = k!$ is a lower bound to this quantity [47], that is, $\mathcal{F}^{(k)}_{\mathrm{Haar}} \leq \mathcal{F}^{(k)}_{\mathcal{E}_H}$ so a larger value of the frame potential means less randomness.

Proposition 4. *The frame potential of $\mathcal{E}_H$ obeys the following lower bound:*

$$\mathcal{F}^{(k)}_{\mathcal{E}_H} \geq d^{-2k} |\mathrm{tr}(U)|^{4k} \tag{18}$$

The above result is useful to see if an ensemble deviates from the Haar distribution, see Appendix C.2 for the proof. Taking the infinite time average $\mathbb{E}_T(\cdot) = \lim_{T\to\infty} T^{-1} \int_0^T (\cdot) dt$ of the r.h.s., we can calculate a lower bound for the asymptotic value of the frame potential.

Proposition 5. *If the spectrum of H is generic:*

$$\mathbb{E}_T \left[d^{-2k} |\mathrm{tr}(U)|^{4k} \right] = (2k)! + O(d^{-1}) \tag{19}$$

As we can see, it is far from the Haar value $k!$. The request for the spectrum being generic is a stronger form of non-resonance; see Appendix C.3 for the definition of generic spectrum and Appendix C.4 for the proof. The infinite time average shows that the asymptotic value is the same for GUE and GDE. On the other hand, the frame potential $\mathcal{F}^{(k)}_{\mathcal{E}_H}$ is non-trivial in its time evolution. For $k = 1$, we have [67]:

$$\mathcal{F}^{(1)}_{\mathcal{E}_H} = \frac{d^2}{(d^2-1)} (d^2 \tilde{c}_4(t) - 2\tilde{c}_2(t) + 1) \tag{20}$$

where of course the coefficients $\tilde{c}_k(t)$ do depend on the spectrum of H. We can now take the ensemble average $\overline{\mathcal{F}^{(1)}_{\mathcal{E}_H}}^E$ of this quantity. The results are plotted in Figure 2. We can see that the behavior of the Poisson and GDE spectra is quite distinct from that of the GUE. Indeed, for the first two ensembles, the frame potential never goes below the asymptotic value $3 + O(d^{-1})$, so it always stays away from the Haar value 1. On the other hand, the frame potential, corresponding to GUE, equals the Haar value 1 in the whole temporal interval $t \in [O(d^{1/3}), O(d)]$.

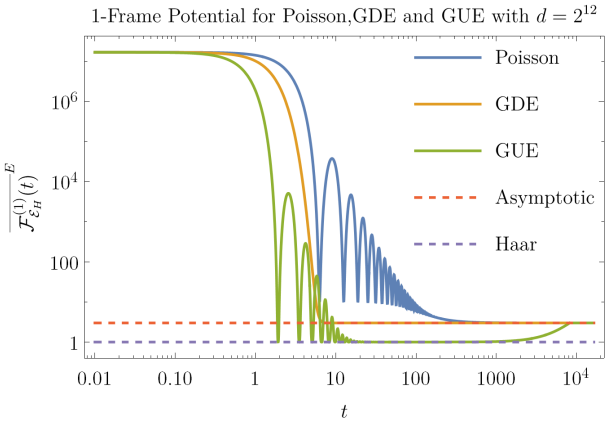

Figure 2. Log–log plot of the ensemble average of $\overline{\mathcal{F}^{(1)}_{\mathcal{E}_H}(t)}^{E}$ for $E \equiv$ GUE, $E \equiv$ GDE and $E \equiv$ P for $d = 2^{12}$. The dashed lines represent the Haar value $\mathcal{F}^{(1)}_{\text{Haar}} = 1$ and the asymptotic value of $\lim_{t\to\infty} \overline{\mathcal{F}^{(1)}_{\mathcal{E}_H}(t)}^{E} = 3 + O(d^{-1})$. Note that at late times $t = O(d)$, $\overline{\mathcal{F}^{(1)}_{\mathcal{E}_H}}^{\text{GUE}}$ distances from the Haar value [54] and reaches the asymptotic value.

Proposition 6. *The ensemble average of the frame potential for $E \equiv$ GDE satisfies:*

$$\overline{\mathcal{F}^{(k)}_{\mathcal{E}_H}}^{GDE} \geq (2k)! + O(d^{-1}) \tag{21}$$

showing that the GDE ensemble is always different from the Haar value.

See Appendix C.5 for the details of the proof.

7. Loschmidt Echo and OTOC

The Loschmidt Echo (LE) is a quantity that captures the sensitivity of the dynamics to small perturbations. In [72,73], it was found that under suitable conditions, the OTOC and LE are quantitatively equivalent. Our aim in this section is to give another insight in that direction, showing that, using the isospectral twirling, the LE assumes the form of an OTOC-like quantity. The LE is defined as the fidelity between quantum states [74–76]; for an infinite temperature state, we have that the LE is $\mathcal{L}(t) = d^{-2}|\text{tr}(e^{iHt}e^{-i(H+\delta H)t})|^2$.

Proposition 7. *Let $A \in \mathcal{U}(\mathcal{H})$ be a unitary operator, provided that $Sp(H) = Sp(H + \delta H)$ the isospectral twirling of the LE is given by:*

$$\langle \mathcal{L}(t) \rangle_G = \text{tr}(\tilde{T}_{(14)(23)} \mathcal{A}^{\otimes 2} \hat{\mathcal{R}}^{(4)}(U)) \tag{22}$$

where $\mathcal{A} := A^\dagger \otimes A$. See Appendix D.1 for the proof. If one sets $\mathcal{A}$ to be a Pauli operator on qubits, one obtains [67]:

$$\langle \mathcal{L}(t) \rangle_G = \tilde{c}_4(t) + d^{-2} + O(d^{-4}) \tag{23}$$

In conclusion, we can say that both LE and OTOC are proportional to the $4-$point spectral form factor in this setting. We can conclude that also the LE is a probe of scrambling; we thus find an agreement with the statement of [54]. Indeed, in proving Equation (22), we give an expression of the LE in terms of the $2-$point auto-correlation function $|\text{tr}(A^\dagger(t)A)|^2$; in [54], it was proved that the decay of the averaged $2-$point autocorrelation function implies the decay of the TMI, i.e., implies scrambling [12,13].

8. Entanglement

We now move on to showing how the isospectral twirling also describes the evolution of entanglement under a random Hamiltonian with a given spectrum. Consider the unitary time evolution of a state $\psi \in \mathcal{B}(\mathcal{H}_A \otimes \mathcal{H}_B)$ by $\psi \mapsto \psi_t \equiv U\psi U^\dagger$. The entanglement of ψ_t in

the given bipartition is computed by the 2−Rényi entropy $S_2 = -\log \mathrm{tr}(\psi_A(t)^2)$, where $\psi_A(t) := \mathrm{tr}_B \psi_t$.

Proposition 8. *The isospectral twirling of the* 2−*Renyi entropy is lower bounded by:*

$$\langle S_2 \rangle_G \geq -\log \mathrm{tr}\Big(T_{(13)(24)} \hat{\mathcal{R}}^{(4)}(U) \psi^{\otimes 2} \otimes T_{(A)} \Big) \tag{24}$$

where $T_{(A)} \equiv T_A \otimes \mathbb{1}_B^{\otimes 2}$ *and* T_A *is the swap operator on* $\mathcal{H}_A$.

See Appendix E.1 for the proof. If one sets $d_A = d_B = \sqrt{d}$, one obtains [67]:

$$\begin{aligned} \langle S_2 \rangle_G \geq & -\log \Big[2d^{-1/2} + \tilde{c_4}(t) \Big(\mathrm{tr}(\psi_A^2) - 2d^{-1/2} \Big) \Big] \\ & + O(1/d) \end{aligned} \tag{25}$$

As the temporal behavior of $\langle S_2 \rangle_G$ is dictated by $\tilde{c_4}(t)$, one expects that entanglement dynamics can also distinguish between chaotic and non-chaotic behavior. The complete analysis of these dynamics is found in [67].

9. Tripartite Mutual Information

The TMI is defined as [12,13] $I_3(A:C:D) := I(A:C) + I(A:D) - I(A:CD)$ where A, B and C, D are fixed bipartitions of past and future time slices of the quantum system after a unitary evolution U; $I(A:C)$ is the mutual information defined through the Von Neumann entropy. Here, we work with the TMI using the 2-Rényi entropy as measure of entropy and denote it by $I_{3_{(2)}}(U) = \log d + \log \mathrm{tr}\rho_{AC}^2 + \log \mathrm{tr}\rho_{AD}^2$; see Appendix F.2. Here, $\rho_{AC(AD)} = \mathrm{tr}_{BD(BC)}(\rho_U)$, where ρ_U is the Choi state [77] of the unitary evolution $U \equiv \exp\{-iHt\}$ and H a random Hamiltonian with a given spectrum. Set $A = C$ and $B = D$, then, by defining $T_{(C)}^U := U^{\otimes 2} T_{(C)} U^{\dagger \otimes 2}$, $I_{3_{(2)}}$ can be written as (see Appendix F.3):

$$I_{3_{(2)}} = -3\log d + \log \mathrm{tr}(T_{(C)}^U T_{(C)}) + \log \mathrm{tr}(T_{(C)}^U T_{(D)}) \tag{26}$$

The second term of Equation (26) is similar to the entanglement of quantum evolutions defined in [78].

Proposition 9. *The isospectral twirling of* $I_{3_{(2)}}$ *is upper bounded by:*

$$\begin{aligned} \left\langle I_{3_{(2)}} \right\rangle_G \leq & \log d + \log \mathrm{tr}(\tilde{T}_{(13)(24)} \hat{\mathcal{R}}^{(4)}(U) T_{(C)}^{\otimes 2}) \\ & + \log \mathrm{tr}(\tilde{T}_{(13)(24)} \hat{\mathcal{R}}^{(4)}(U) T_{(C)} \otimes T_{(D)}) \end{aligned} \tag{27}$$

Since the TMI is a negative-definite quantity, the decay of the r.h.s. of Equation (27) implies scrambling, i.e., the l.h.s. drops closer to its minimum value. The tightness of this bound deserves further investigations. By explicitly computing Equation (27), one has [67]:

$$\begin{aligned} \left\langle I_{3_{(2)}}(t) \right\rangle_G \leq & \log_2(2 - 3\tilde{c_4}(t) + 2\mathrm{Re}\tilde{c_3}(t)) \\ & + \log_2(\tilde{c_4}(t) + (2 - \tilde{c_4}(t))d^{-1}) + O(d^{-2}) \end{aligned} \tag{28}$$

We can now compute $\overline{\left\langle I_{3_{(2)}} \right\rangle_G}^E$ over the spectra GUE, GDE and Poisson. We set $d_C = \dim(\mathcal{H}_C)$ and $d_D = \dim \mathcal{H}_D$ and $d_C = d_D = \sqrt{d}$. The time evolution of $\overline{\left\langle I_{3_{(2)}} \right\rangle_G}^E$ depends on the spectral form factors. We can see in Figure 3 how the chaotic and integrable behaviors

are clearly different. The salient timescales of $I_{3_{(2)}}(t)$ depend on the timescales of $\tilde{c}_4(t)$[67]. The plateau values of Equation (28) are, for large d:

$$\lim_{t\to\infty} \overline{\left\langle I_{3_{(2)}}(t)\right\rangle_G}^E = 2 - \log_2 d + O(d^{-1}) \tag{29}$$

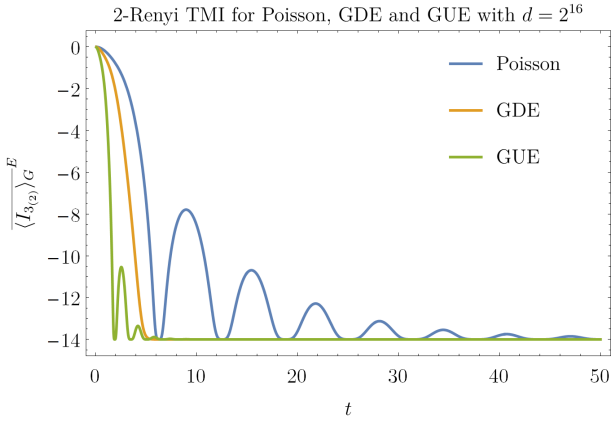

Figure 3. Plot of the upper bound for $\overline{\left\langle I_{3_{(2)}}(t)\right\rangle_G}^E$, see r.h.s of Equation (27), for E ≡ P, E ≡ GUE and E ≡ GDE with $d_C = d_D = d^{1/2}$ and $d = 2^{16}$. GUE and Poisson reveal oscillations before the plateau whose amplitude and damp time increases with the system size d, see Equations (29) and (30), respectively. For GDE there are no oscillations: the plateau is reached in $O(\sqrt{\log d})$.

One thing to note is that the fluctuations of GUE and Poisson decay in time

$$t_{\text{fluct}} = \alpha + \beta \log d \tag{30}$$

where the parameters α, β for the different ensembles are GUE: $\alpha = -3.9, \beta = 0.8$ Poisson $\alpha = -16.3, \beta = 3.2$.

10. Conclusions and Outlook

Chaos is an important subject in quantum many-body physics, and the understanding of its appearance is of fundamental importance for a number of situations ranging from quantum information algorithms to black hole physics. In this paper, we unified the plethora of probes to quantum chaos in the notion of isospectral twirling. Since this quantity depends explicitly on the spectrum of the Hamiltonian, one can compare its behavior for different spectra characterizing chaotic and non-chaotic behavior, which we did by using random matrix theory. We demonstrate how different temporal features depend on the interplay between spectrum and eigenvectors of the Hamiltonian. Random eigenvectors obtained with Clifford resources result in markedly different asymptotic values of the OTOCs. Moreover, a doping of Clifford circuits with non-Clifford resources interpolates the long time scaling of the OTOCs between a class of integrable models and quantum chaos.

In perspective, there are several open questions. First and foremost, we want to extend the results of the crossover to more structural aspects of the dynamics with the goal of obtaining a quantum KAM theorem. Second, one could systematically study how different spectra behave together with different ensembles of eigenvectors, for instance, interpolating between Clifford and universal resources in a random quantum circuit [79], by doping a stabilizer Hamiltonian with non-Clifford resources such as the $T-$gates [66]. Another important aspect is that of the locality of the interactions. In this work, we did not take into account the locality of interactions. Locality might result in even more striking differences in the onset of quantum chaotic behavior. In this paper, we have treated the spectrum and the eigenvectors of the Hamiltonian separately, showing how they both contribute to

quantum chaotic features. This is possible because in the spectral resolution, spectrum and eigenvectors are distinct. However, in realistic systems, we often find that *both spectra and eigenvectors* possess quantum chaotic features; this should depend on the fact that we deal with local Hamiltonians. Through the connections found with entanglement and quantum thermodynamics, one also hopes to exploit these findings to design more efficient quantum batteries. Finally, the notion of isospectral twirling could be generalized to non-unitary quantum channels and used to study chaotic behavior in open quantum systems.

Author Contributions: Data curation, S.F.E.O.; Investigation, L.L., S.F.E.O. and A.H.; Methodology, L.L., S.F.E.O. and A.H.; Supervision, A.H. All authors have read and agreed to the published version of the manuscript.

Funding: This research was funded by National Science Foundation grant number 2014000.

Acknowledgments: We acknowledge support from NSF award number 2014000. We thank F. Caravelli for enlightening discussions.

Conflicts of Interest: The authors declare no conflict of interest.

Appendix A. $4k-$Point OTOC

Appendix A.1. Proof of Proposition 1

Recall definition (6) and use the cyclic property of the trace to write it in terms of $B_l(-t) = UB_lU^\dagger$:

$$\begin{aligned}\mathrm{OTOC}_{4k} = \frac{1}{d}\mathrm{tr}(&A_1^\dagger B_1^\dagger(-t)\cdots A_k^\dagger B_k^\dagger(-t)\times\\ &A_1B_1(-t)\cdots A_kB_k(-t))\end{aligned} \tag{A1}$$

to write the product of operators in terms of a tensor product, let us use the property proven in [67]:

$$\begin{aligned}\mathrm{OTOC}_{4k} = \mathrm{tr}(&\tilde{T}_{1\,4k\cdots 2}(A_1^\dagger\otimes B_1^\dagger\otimes\cdots\otimes A_k\otimes B_k)\times\\ &(U\otimes U^\dagger)^{\otimes 2k})\end{aligned} \tag{A2}$$

where $(1\,4k\cdots 2)\in S_{4k}$. Now let us act with the adjoint action of $S := \prod_{l=0}^{k-1} T_{(2l+2\;2k+2l+1)}$, $(2l+2\;2k+2l+1)\in S_{4k}$ on $(U\otimes U^\dagger)^{\otimes 2k}$; inserting multiple $S^\dagger S\equiv \mathbb{1}$ one obtains:

$$\mathrm{OTOC}_{4k} = \mathrm{tr}\Big(\tilde{T}_\pi^{(4k)}(A_1^\dagger\otimes A_1\otimes\cdots\otimes B_k^\dagger\otimes B_k)U^{\otimes k,k}\Big) \tag{A3}$$

where $\tilde{T}_\pi^{(4k)} = S\tilde{T}_{1\,4k\cdots 2}S^\dagger$; defining $\mathcal{A}_l = \otimes_{l=1}^k A_l^\dagger\otimes A_l$, similarly for $\mathcal{B}$ and averaging over $U_G := G^\dagger UG$ one obtains the desired result (7).

Appendix A.2. Proof of Equation (10)

Setting $k=1$, we have $T_\pi^{(4)} = T_{(23)}T_{(1432)}T_{(23)} = T_{(1423)}$; therefore, Equation (A3) after the isospectral twirling reads:

$$\mathrm{OTOC}_4 = \mathrm{tr}\Big(T_{(1423)}(\mathcal{A}\otimes\mathcal{B})R^{(4)}(U)\Big) \tag{A4}$$

this concludes the proof.

Appendix B. Calculations for the Clifford Averages

Appendix B.1. Calculation of $\mathrm{tr}(U_\infty^{\otimes 2,2} Q T_\sigma)$

Defining $\Pi_{ijij} \equiv \Pi_i \otimes \Pi_j \otimes \Pi_i \otimes \Pi_j$ and similarly for the others, $U_\infty^{\otimes 2,2}$ reads:

$$U_\infty^{\otimes 2,2} = \sum_{i \neq j} (\Pi_{ijij} + \Pi_{ijji}) + \sum_i \Pi_{iiii} \tag{A5}$$

Then, let us split Q into two parts:

$$Q = \frac{\mathbb{1}^{\otimes 4}}{d^2} + \sum_{P \neq \mathbb{1}} P^{\otimes 4} \equiv \frac{\mathbb{1}^{\otimes 4}}{d^2} + Q' \tag{A6}$$

We write:

$$\mathrm{tr}(U_\infty^{\otimes 2,2} Q T_\sigma) = \frac{1}{d^2} \mathrm{tr}(U^{\otimes 2,2} T_\sigma) + \mathrm{tr}(U_\infty^{\otimes 2,2} Q' T_\sigma) \tag{A7}$$

and note that the first part coincides with the asymptotic values of these traces used for the computation of the usual Isospectral twirling, see [67]:

$$\mathrm{tr}(U_\infty^{\otimes 2,2} Q T_\sigma) = \frac{1}{d^2} \mathrm{tr}(U^{\otimes 2,2} T_\sigma) + \mathrm{tr}(U_\infty^{\otimes 2,2} Q' T_\sigma) \tag{A8}$$

the only part that are left out and need evaluation is $\mathrm{tr}(U_\infty^{\otimes 2,2} Q' T_\sigma)$, with $Q' = \sum_{P \neq \mathbb{1}} P^{\otimes 4}$ Therefore, plugging Equation (A5), we find:

$$\begin{aligned}
d^2 \mathrm{tr}(U_\infty^{\otimes 2,2} Q') &= 2d(d-1)^2 + d(d-1) \\
d^2 \mathrm{tr}(U_\infty^{\otimes 2,2} Q' T_{(12)}) &= \mathrm{tr}(U_\infty^{\otimes 2,2} Q' T_{(34)}) \\
&= d(d-1) \\
d^2 \mathrm{tr}(U_\infty^{\otimes 2,2} Q' T_{(23)}) &= \mathrm{tr}(U_\infty^{\otimes 2,2} Q' T_{(24)}) \\
&= \mathrm{tr}(U_\infty^{\otimes 2,2} Q' T_{(13)}) \\
&= \mathrm{tr}(U_\infty^{\otimes 2,2} Q' T_{(14)}) \\
&= d(d-1)^2 + d(d-1) \\
d^2 \mathrm{tr}(U_\infty^{\otimes 2,2} Q' T_{(ijk)}) &= d(d-1) \\
d^2 \mathrm{tr}(U_\infty^{\otimes 2,2} Q' T_{(1234)}) &= \mathrm{tr}(U_\infty^{\otimes 2,2} Q' T_{(1432)}) \\
&= \mathrm{tr}(U_\infty^{\otimes 2,2} Q' T_{(1243)}) \\
&= \mathrm{tr}(U_\infty^{\otimes 2,2} Q' T_{(1342)}) \\
&= d^2(d-1) + d(d-1) \\
d^2 \mathrm{tr}(U_\infty^{\otimes 2,2} Q' T_{(1324)}) &= \mathrm{tr}(U_\infty^{\otimes 2,2} Q' T_{(1423)}) \\
&= d(d-1) \\
d^2 \mathrm{tr}(U_\infty^{\otimes 2,2} Q' T_{(12)(34)}) &= 2d^2(d-1) + d(d-1) \\
d^2 \mathrm{tr}(U_\infty^{\otimes 2,2} Q' T_{(13)(24)}) &= \mathrm{tr}(U_\infty^{\otimes 2,2} Q' T_{(14)(23)}) \\
&= d^2(d-1) + d(d-1)^2 \\
&\quad + d(d-1)
\end{aligned} \tag{A9}$$

The above calculations are straightforward, let us just give some insights and examples. For Π_{iiii}, the result is always the same, indeed $T_\sigma \Pi_{iiii} = \Pi_{iiii}$ and:

$$\begin{aligned}
d^2 \sum_i \mathrm{tr}(\Pi_{iiii} Q) &= \sum_{i, P \neq \mathbb{1}} |\langle i|P|i\rangle|^4 \\
&= \sum_i \sum_{P \ni \{Z,I\} \neq \mathbb{1}} = d(d-1)
\end{aligned} \tag{A10}$$

Or let us calculate $\sum_{i\neq j}\mathrm{tr}(\Pi_{ijij}QT_{(1234)})$:

$$\begin{aligned} d^2\sum_{i\neq j}\mathrm{tr}(\Pi_{ijij}QT_{(1234)}) &= \sum_{i\neq j,P\neq\mathbb{1}}\langle ijij|P|jiji\rangle \\ &= \sum_{i\neq j,P\neq\mathbb{1}}|\langle i|P|j\rangle|^4 \\ &= \sum_{i\neq j,P\neq\mathbb{1}} = d^2(d-1) \end{aligned} \tag{A11}$$

Indeed for any pair of (i,j) with $i\neq j$, there are d Pauli operators, which transform i into j and vice versa. While for $Q^\perp$, we have:

$$\mathrm{tr}(U_\infty^{\otimes 2,2}Q^\perp T_\sigma) = \frac{d^2-1}{d^2}\mathrm{tr}(U^{\otimes 2,2}T_\sigma) - \mathrm{tr}(U_\infty^{\otimes 2,2}Q'T_\sigma) \tag{A12}$$

Appendix B.2. Calculation of $\mathrm{tr}(\tilde{T}_{(1423)}\mathcal{A}\otimes\mathcal{B}QT_\pi)$

Let us calculate this trace for all $\pi\in S_4$:

$$\begin{aligned} \mathrm{tr}(\tilde{T}_{(1423)}\mathcal{A}\otimes\mathcal{B}Q\mathbb{1}) &= \mathrm{tr}(\tilde{T}_{(1423)}\mathcal{A}\otimes\mathcal{B}QT_{(ij)(kl)}) \\ &= d^{-1}\mathrm{tr}(ABAB) = 1 \\ \mathrm{tr}(\tilde{T}_{(1423)}\mathcal{A}\otimes\mathcal{B}QT_{(12)}) &= \mathrm{tr}(\tilde{T}_{(1423)}\mathcal{A}\otimes\mathcal{B}QT_{(34)}) \\ &= \mathrm{tr}(\tilde{T}_{(1423)}\mathcal{A}\otimes\mathcal{B}QT_{(ijk)}) \\ &= \mathrm{tr}(\tilde{T}_{(1423)}\mathcal{A}\otimes\mathcal{B}QT_{(1324)}) \\ &= \mathrm{tr}(\tilde{T}_{(1423)}\mathcal{A}\otimes\mathcal{B}QT_{(1423)}) = 0 \\ \mathrm{tr}(\tilde{T}_{(1423)}\mathcal{A}\otimes\mathcal{B}QT_{(13)}) &= \mathrm{tr}(\tilde{T}_{(1423)}\mathcal{A}\otimes\mathcal{B}QT_{(23)}) \\ &= \mathrm{tr}(\tilde{T}_{(1423)}\mathcal{A}\otimes\mathcal{B}QT_{(14)}) \\ &= \mathrm{tr}(\tilde{T}_{(1423)}\mathcal{A}\otimes\mathcal{B}QT_{(24)}) \\ &= \mathrm{tr}(\tilde{T}_{(1423)}\mathcal{A}\otimes\mathcal{B}QT_{(1234)}) \\ &= \mathrm{tr}(\tilde{T}_{(1423)}\mathcal{A}\otimes\mathcal{B}QT_{(1342)}) \\ &= \mathrm{tr}(\tilde{T}_{(1423)}\mathcal{A}\otimes\mathcal{B}QT_{(1243)}) \\ &= \mathrm{tr}(\tilde{T}_{(1423)}\mathcal{A}\otimes\mathcal{B}QT_{(1432)}) \\ &= d^{-2}\mathrm{tr}(ABAB) = d^{-1} \end{aligned} \tag{A13}$$

The above calculations are straightforward, but let us discuss just one example:

$$\begin{aligned} \mathrm{tr}(\tilde{T}_{(1423)}\mathcal{A}\otimes\mathcal{B}QT_{(1324)}) &= d^{-1}\mathrm{tr}(\mathcal{A}\otimes\mathcal{B}Q) \\ &= d^{-3}\sum_P \mathrm{tr}(AP)^2\mathrm{tr}(BP)^2 \\ &= d\sum_P \delta_{AP}\delta_{BP} = 0 \end{aligned} \tag{A14}$$

since A and B are non-overlapping Pauli operators.

Appendix C. Frame Potential

Appendix C.1. Proof of Proposition 3

Recall the definition of the frame potential

$$\mathcal{F}^{(k)}_{\mathcal{E}_H} = \int dG_1 dG_2 \left|\mathrm{tr}\left(G_1^\dagger U^\dagger G_1 G_2^\dagger U G_2\right)\right|^{2k} \tag{A15}$$

Then:

$$\begin{aligned}\mathcal{F}_{\mathcal{E}_H}^{(k)} &= \int dG_1 dG_2 \mathrm{tr}\Big(G_1^\dagger U G_1 G_2^\dagger U^\dagger G_2\Big)^k \\ &\times \mathrm{tr}\Big(G_1^\dagger U^\dagger G_1 G_2^\dagger U G_2\Big)^k \end{aligned} \tag{A16}$$

Using the property of the trace for which $\mathrm{tr}(A)^k = \mathrm{tr}(A^{\otimes k})$, we can rewrite it as:

$$\mathcal{F}_{\mathcal{E}_H}^{(k)} = \int dG_1 dG_2 \mathrm{tr}\Big(G_1^{\dagger\otimes 2k} U^{\dagger\otimes k,k} G_1^{\otimes 2k} G_2^{\dagger\otimes 2k} U^{\otimes k,k} G_2^{\otimes 2k}\Big) \tag{A17}$$

where $U^{\otimes k,k} \equiv U^{\otimes k} \otimes U^{\dagger\otimes k}$. From the Definition (1), we have:

$$\mathcal{F}_{\mathcal{E}_H}^{(k)} = \mathrm{tr}\Big(\hat{\mathcal{R}}^{(2k)^\dagger}(U)\hat{\mathcal{R}}^{(2k)}(U)\Big) = \|\hat{\mathcal{R}}^{(2k)}(U)\|_2^2 \tag{A18}$$

the result is proven. To write $\mathcal{F}_{\mathcal{E}_H}^{(k)}$ in a linear form, define $T_{1\leftrightarrow 2} \equiv \prod_{l=1}^{2k} T_{(l\,2k+l)}$:

$$\mathcal{F}_{\mathcal{E}_H}^{(k)} = \mathrm{tr}\Big(T_{1\leftrightarrow 2}\Big(\hat{\mathcal{R}}^{(2k)^\dagger} \otimes \hat{\mathcal{R}}^{(2k)}\Big)\Big) \tag{A19}$$

Appendix C.2. Proof of Proposition 4

In order to prove Proposition 4, we make use the usual bound holding for the Schatten p-norms [80] $\|A\|_p \leq \mathrm{rank}(A)^{\frac{1}{p}-\frac{1}{q}}\|A\|_q$. Since $\mathrm{rank}(A) = \mathrm{rank}(A^\dagger A)$, we have $\mathrm{rank}(\hat{\mathcal{R}}^{(2k)}(U)) = d^{2k}$ and thus:

$$\|\hat{\mathcal{R}}^{(2k)}(U)\|_2 \geq \frac{\|\hat{\mathcal{R}}^{(2k)}(U)\|_1}{d^k} \geq \frac{\Big|\mathrm{tr}(\hat{\mathcal{R}}^{(2k)}(U))\Big|}{d^k} \tag{A20}$$

where we used the property $|\mathrm{tr}(A)| \leq \|A\|_1$, which can be derived from [80] $|\mathrm{tr}(AB)| \leq \|A\|_p\|B\|_q$ where $p^{-1}+q^{-1}=1$, setting $B \equiv \mathbb{1}$, $p=1$ and $q=\infty$. Finally, we obtain:

$$\mathcal{F}_{\mathcal{E}_H}^{(k)} \geq \frac{\Big|\mathrm{tr}(\hat{\mathcal{R}}^{(2k)}(U))\Big|^2}{d^{2k}} \tag{A21}$$

Just recalling that $\mathrm{tr}(\hat{\mathcal{R}}^{(2k)}(U)) = |\mathrm{tr}(U)|^{2k}$, we obtain the desired bound (3).

Appendix C.3. Definition of Generic Spectrum

Given $\{E_n\}_{n=1}^d$, the spectrum of a Hamiltonian H on $\mathcal{H} \simeq \mathbb{C}^d$, it is said to be *generic* iff for any $d \geq l \geq 1$:

$$\sum_{m=i}^{l} E_{n_i} - \sum_{j=1}^{l} E_{m_j} \neq 0 \tag{A22}$$

unless $E_{n_i} = E_{m_j}, \forall i,j = 1,\ldots,l$ and for some permutation of the indices n_i, m_j.

Appendix C.4. Proof of Proposition 5

We need to compute the infinite time average of $|\mathrm{tr}(U)|^{4k}$. Let us write the unitary with its spectral decomposition: $U = \sum_k e^{iE_k t}\Pi_k$, assuming $\{E_i\}_{i=1}^d$ is a generic spectrum:

$$|\mathrm{tr}(U)|^{4k} = \sum_{\substack{m_1\ldots m_{2k} \\ n_1\ldots n_{2k}}} \exp\left\{ it\sum_{i=1}^{2k} E_{m_i} - it\sum_{j=1}^{2k} E_{n_j} \right\} \tag{A23}$$

Taking the infinite time average, the result is zero unless $E_{m_i} = E_{n_j}$ for all i, j:

$$\begin{aligned}\overline{|\mathrm{tr}(U)|^{4k}}^T &= \sum_{\text{pairs}} \sum_{m_1 \dots m_{2k}} \sum_{n_1 \dots n_{2k}} \delta_{i_1 j_1} \cdots \delta_{i_{2k} j_{2k}} + \text{error} \\ &= \sum_{\text{pairs}} d^{2k} + \text{error} = (2k)! d^{2k} + O(d^{2k-1})\end{aligned} \tag{A24}$$

the error comes from the fact that we over-count the pairs, e.g., the case $\delta_{i_1 j_1}\delta_{i_2 j_2}$ overlaps with $\delta_{i_1 j_2}\delta_{i_2 j_1}$ because we are considering the case $\delta_{i_1 j_1}\delta_{i_1 j_2}\delta_{i_2 j_1}\delta_{i_2 j_2}$ twice; thus, the error is $O(d^{2k-1})$. After these considerations, we obtain:

$$\frac{\overline{|\mathrm{tr}(U)|^{4k}}^T}{d^{2k}} = (2k)! + O(d^{-1}) \tag{A25}$$

Appendix C.5. Proof of Proposition 6

The k-th frame potential of the ensemble $\mathcal{E}_H$ is lower bounded by $|\mathrm{tr}(U)|^{4k}/d^{2k}$, recall (3). Now we should prove that:

$$\frac{\overline{|\mathrm{tr}(U)|^{4k}}^{\mathrm{GDE}}}{d^{2k}} \geq (2k)! + O(d^{-1}) \tag{A26}$$

So:

$$|\mathrm{tr}(U)|^{4k} = \sum_{\substack{m_1 \dots m_{2k} \\ n_1 \dots n_{2k}}} \exp\left\{ it \sum_{i=1}^{2k} E_{m_i} - it \sum_{j=1}^{2k} E_{n_j} \right\} \tag{A27}$$

Let us exclude from this sum all the terms, such that $E_{m_i} = E_{n_j}$ for any pairs:

$$\begin{aligned}\frac{|\mathrm{tr}(U)|^{4k}}{d^{2k}} &= (2k)! \\ &+ d^{-2k} \sum_{\substack{m_1 \neq n_1, \dots, n_{2k} \\ \dots\dots\dots\dots\dots\dots \\ m_{2k} \neq n_1, \dots, n_{2k}}} \exp\left\{ it \sum_{i=1}^{2k} E_{m_i} - it \sum_{j=1}^{2k} E_{n_j} \right\} \\ &+ O(d^{-1})\end{aligned} \tag{A28}$$

see Appendix C.4 for a discussion regarding the error $O(d^{-1})$. After the ensemble average over GDE [67], the second term of the above equation returns a sum of Fourier transforms of Gaussians weighted by positive coefficients depending on the dimension d. Hence:

$$\frac{|\mathrm{tr}(U)|^{4k}}{d^{2k}} \geq (2k)! + O(d^{-1}) \tag{A29}$$

This concludes the proof.

Appendix D. Loschmidt Echo

Appendix D.1. Proof of Proposition 7

We first show that when the perturbation of H leaves the spectrum unchanged, $\mathrm{Sp}(H) = \mathrm{Sp}(H + \delta H)$, then $\mathcal{L}(t)$ can be viewed as a two-point auto-correlation function. Any perturbation that leaves the spectrum unchanged can be viewed as a perturbation

obtained by rotating the Hamiltonian by a unitary operator close to the identity, say $A \in \mathcal{U}(\mathcal{H})$, $H + \delta H = A^\dagger H A$; one obtains:

$$\begin{aligned} \mathcal{L}(t) &= d^{-2}|\mathrm{tr}(e^{iHt}e^{-iA^\dagger HAt})|^2 \\ &= d^{-2}|\mathrm{tr}(e^{iHt}A^\dagger e^{-iHt}A)|^2 \end{aligned} \tag{A30}$$

in the last equality, we have used the unitarity of A and the series of $e^{iHt} = \sum_n \frac{(it)^n}{n!}H^n$. Twirling the unitary evolution with G, $U_G = G^\dagger \exp\{-iHt\}G$ and using $\mathrm{tr}(A)\mathrm{tr}(B) = \mathrm{tr}(A \otimes B)$, one can easily express:

$$\mathcal{L}(t) = d^{-2}\mathrm{tr}(U_G^{\otimes 2}(A \otimes A^\dagger)U_G^{\dagger\otimes 2}(A^\dagger \otimes A)) \tag{A31}$$

It is straightforward to verify $\mathrm{tr}(T_{(13)(24)}A^{\otimes 2} \otimes B^{\otimes 2}) = \mathrm{tr}(A^{\otimes 2}B^{\otimes 2})$ and express

$$\mathcal{L}(t) = \mathrm{tr}(T_{(13)(24)}(U_G^{\otimes 2} \otimes U_G^{\dagger\otimes 2})A \otimes A^\dagger \otimes A^\dagger \otimes A) \tag{A32}$$

Inserting $T^2_{(13)(24)} \equiv \mathbb{1}$, one obtains:

$$\mathcal{L}(t) = \mathrm{tr}(T_{(13)(24)}(A^\dagger \otimes A \otimes A \otimes A^\dagger)(U_G^{\otimes 2} \otimes U_G^{\dagger\otimes 2})) \tag{A33}$$

Inserting $T^2_{(12)} \equiv \mathbb{1}$ and noting that $[T_{(12)}, (U_G^{\otimes 2} \otimes U_G^{\dagger\otimes 2})] = 0$, we finally obtain (10).

Appendix E. Entanglement

Appendix E.1. Proof of Proposition 8

Starting from the definition of 2−Rényi entropy, through the identity $\mathrm{tr}_A(\mathcal{O}_A^2) = \mathrm{tr}(\mathcal{O}_A^{\otimes 2}T_{(A)})$, where $T_{(A)} \equiv T_A \otimes \mathbb{1}_B^{\otimes 2}$ and T_A is the swap operator, it is possible to express the 2−Rényi entropy as:

$$S_2 = -\log \mathrm{tr}\Big[T_{(A)}U^{\otimes 2}\psi^{\otimes 2}U^{\dagger\otimes 2}\Big] \tag{A34}$$

Again, we average over the isospectral unitary evolutions by $U \mapsto G^\dagger U G$ and obtain

$$\begin{aligned} \langle S_2\rangle_G &= \langle -\log \mathrm{tr}\Big[T_{(A)}U^{\otimes 2}\psi^{\otimes 2}U^{\dagger\otimes 2}\Big]\rangle_G \\ &\geq -\log \mathrm{tr}\Big[T_{(A)}\langle U^{\otimes 2}\psi^{\otimes 2}U^{\dagger\otimes 2}\rangle_G\Big] \end{aligned} \tag{A35}$$

where the lower bound follows by the Jensen inequality by the concavity of the function $-\log$. Now, calling $a \equiv U^{\otimes 2}\psi^{\otimes 2}$, $b \equiv U^{\dagger\otimes 2}T_{(A)}$, and using $\mathrm{tr}[ab] = \mathrm{tr}[T_{(13)(24)}a \otimes b]$, we obtain

$$\langle S_2\rangle_G \geq -\log \mathrm{tr}\Big[T_{(13)(24)}\hat{\mathcal{R}}^{(4)}(U)\psi^{\otimes 2} \otimes T_{(A)}\Big] \tag{A36}$$

Appendix F. Tripartite Mutual Information

Appendix F.1. Choi State: Definition and Properties

Let $U \in \mathcal{U}(\mathcal{H})$ be a unitary operator, which decomposed in a basis $\{|i\rangle\}$ reads $U = \sum_{i,j} u_{ij}|i\rangle\langle j|$. The Choi isomorphism maps an operator $\mathcal{O}$ into a state $|\mathcal{O}\rangle \in \mathcal{B}(\mathcal{H}^{\otimes 2})$. The two copies $\mathcal{H}^{\otimes 2}$ of the Hilbert space can be thought of as one lying in the past (input), the other in the future (output) [12]. The normalized state corresponding to U reads:

$$|U\rangle = d^{-1/2}\sum_{ij} u_{ji}|i\rangle \otimes |j\rangle \tag{A37}$$

note that defined $|I\rangle$ as the bell state between the two copies of $\mathcal{H}$: $|I\rangle = \frac{1}{\sqrt{d}}\sum_i |i\rangle \otimes |i\rangle$ one has $|U\rangle = (\mathbb{1} \otimes U)|I\rangle$. The density matrix associated with the Choi state of U:

$$\rho_U = |U\rangle\langle U| = (\mathbb{1} \otimes U)|I\rangle\langle I|(\mathbb{1} \otimes U^\dagger) \tag{A38}$$

One important property is that if one traces out the input (output), the resulting state is always maximally mixed. This reflects the idea that the input and the output are always maximally entangled. Here, we can prove a slightly stronger statement.

Proposition A1. *Let f be a trace preserving, unital $CP-$map; the Choi state $\rho_f = \mathbb{1} \otimes f(|I\rangle\langle I|)$ is such that:*

$$\mathrm{tr}_{1(2)}(\rho_f) \propto \mathbb{1}_{2(1)} \tag{A39}$$

where the subscript $1(2)$ indicates the first (second) copy of $\mathcal{H}$.

Proof. Let us first prove the statement for 1. Writing ρ_f explicitly and tracing out the input we obtain $\mathrm{tr}_1(\rho_f) = d^{-1}\sum_{ij}\mathrm{tr}(|i\rangle\langle j|_1) \otimes f(|i\rangle\langle j|_2)$ from which one obtains $\mathrm{tr}_1(\rho_f) \propto f(\mathbb{1})$, which is the identity since f is unital. To prove the statement for 2, we need f to be trace preserving: $\mathrm{tr}_2(\rho_f) = d^{-1}\sum_{ij}|i\rangle\langle j|_1 \otimes \mathrm{tr}(f(|i\rangle\langle j|_2)) = d^{-1}\mathbb{1}$, which concludes the proof. This proposition is important for our purposes: it ensures that taking the average over an ensemble of unitaries, $\mathcal{E}_H$ in particular, preserves the properties of the Choi state. □

Appendix F.2. 2−Rényi TMI

Consider a unitary time evolution $U_{AB\to CD}$, where A, B and C, D are fixed bipartitions of dimensions $d_A, \ldots, d_D$ of past and future time slices of the quantum system: $(\mathcal{H}_A \otimes \mathcal{H}_B) \otimes (\mathcal{H}_C \otimes \mathcal{H}_D)$. The TMI defined through $2-$Rényi entropy reads [12,13]:

$$I_{3_{(2)}} = S_2(C) + S_2(D) - S_2(AC) - S_2(AD) \tag{A40}$$

from the hierarchy of Rényi entropy follows $I_3 \leq I_{3_{(2)}}$, where I_3 is the TMI calculated with the Von Neumann entropy. For the Choi state of $U_{AB\to CD}$, ρ_U, we have:

$$I_{3_{(2)}} = \log d + \log \mathrm{tr}(\rho_{AC}^2) + \log \mathrm{tr}(\rho_{AD}^2) \tag{A41}$$

where $\rho_{AC(AD)} = \mathrm{tr}_{BD(BC)}(\rho_U)$. It is straightforward to see that $I_{3_{(2)}}$ has the following bounds:

$$-2\log d_A \leq I_{3_{(2)}} \leq 0 \tag{A42}$$

the lower bound is achieved when the information has scrambled, while the upper bound is achieved in the opposite case.

Proposition A2. *The unitaries of the type $\tilde{U} = U_C \otimes U_D$, where $U_C \in \mathcal{U}(\mathcal{H}_C)$, $U_D \in \mathcal{U}(\mathcal{H}_D)$, satisfy:*

$$I_{3_{(2)}}(\tilde{U}) = 0 \tag{A43}$$

therefore, according to this measure of scrambling, do not scramble the information.

Proof. First rewrite Equation (A41) as

$$I_{3_{(2)}} = \log d + \log \mathrm{tr}\left(\rho^{\otimes 2} T_{(A)} T_{(C)}\right) + \log \mathrm{tr}\left(\rho^{\otimes 2} T_{(A)} T_{(D)}\right) \tag{A44}$$

where $T_{(A)} \equiv T_A \otimes \mathbb{1}_{BCD}^{\otimes 2}$ and T_A the swap operator on $\mathcal{H}_A$, similarly for $T_{(C)}$ and $T_{(D)}$. The Choi state of $\tilde{U}$:

$$\rho_{\tilde{U}} = (\mathbb{1}_{AB} \otimes U_C \otimes U_D)|I\rangle\langle I|(\mathbb{1}_{AB} \otimes U_C \otimes U_D)^\dagger \tag{A45}$$

Inserting it into Equation (A44), making use of the cyclic property of the trace and exploting the fact that $[U_{C(D)}, T_{D(C)}] = 0$, one obtains:

$$\begin{aligned} I_{3_{(2)}}(\tilde{U}) = \log d + \log \mathrm{tr}\Big(|I\rangle\langle I|^{\otimes 2} T_{(A)} U_C^{\dagger\otimes 2} T_{(C)} U_C^{\otimes 2}\Big) \\ + \log \mathrm{tr}\Big(|I\rangle\langle I|^{\otimes 2} T_{(A)} U_D^{\dagger\otimes 2} T_{(D)} U_D^{\otimes 2}\Big) \end{aligned} \tag{A46}$$

since $\left[U_C^{\otimes 2}, P_C\right] = 0$, and $\left[U_D^{\otimes 2}, P_D\right] = 0$, we obtain

$$\begin{aligned} I_{3_{(2)}}(\tilde{U}) = \log d + \log \mathrm{tr}\Big(|I\rangle\langle I|^{\otimes 2} T_{(A)} T_{(C)}\Big) \\ + \log \mathrm{tr}\Big(|I\rangle\langle I|^{\otimes 2} T_{(A)} T_{(D)}\Big) \end{aligned} \tag{A47}$$

at this point a straightforward calculation shows that $I_{3_{(2)}}(\tilde{U}) = 0$. □

Appendix F.3. Proof of Equation (26) and Proposition 9

We start from Equation (A41) and rewrite it as Equation (A44), where $\rho_U = (\mathbb{1}_{AB} \otimes U_{CD})|I\rangle\langle I|(\mathbb{1}_{AB} \otimes U_{CD}^{\dagger})$. Let us set $A = C$ and $B = D$. We need two facts. First, note that in this setting $|I\rangle\langle I| = \psi_{AC} \otimes \psi_{BD}$, where ψ_{AC}, ψ_{BD} are Bell states. Second, let T be the swap operator and let $\psi \in \mathcal{H}$ be a pure state, then $T\psi^{\otimes 2} = \psi^{\otimes 2}$. Now let us focus on the second term of Equation (A44). Using the above identity, we have:

$$T_{(A)} T_{(C)} \psi_{AC}^{\otimes 2} = \psi_{AC}^{\otimes 2} \implies T_{(A)} \psi_{AC}^{\otimes 2} = T_{(C)} \psi_{AC}^{\otimes 2} \tag{A48}$$

In this way, we can trace out $\mathcal{H}_A \otimes \mathcal{H}_B$ and obtain that:

$$\log \mathrm{tr}\Big(\rho_U^{\otimes 2} T_{(A)} T_{(C)}\Big) = d^{-2} \log \mathrm{tr}\Big(U_{CD}^{\otimes 2} T_{(C)} U_{CD}^{\dagger\otimes 2} T_{(C)}\Big) \tag{A49}$$

where the factor d^{-2} comes from having traced out the Bell states $\mathrm{tr}_{A(B)}(\psi_{AC(BD)}^{\otimes 2}) = d_{C(D)}^{-2} \mathbb{1}_{C(D)}$. For the second term in Equation (A44), we can play the same game and obtain:

$$\log \mathrm{tr}\Big(\rho_U^{\otimes 2} T_{(A)} T_{(D)}\Big) = d^{-2} \log \mathrm{tr}\Big(U_{CD}^{\otimes 2} T_{(C)} U_{CD}^{\dagger\otimes 2} T_{(D)}\Big) \tag{A50}$$

to prove Equation (27), we use $\mathrm{tr}(ab) = \mathrm{tr}(T_{(13)(24)} a \otimes b)$ if $a, b \in \mathcal{H}^{\otimes 2}$, then we take the isospectral twirling over $U_G = G^{\dagger} \exp\{-iHt\} G$ and use the Jensen inequality to upper bound $I_{3_{(2)}}$.

References

1. Lloyd, S. Black Holes, Demons and the Loss of Coherence: How Complex Systems Get Information, and What They Do with It. Ph.D. Thesis, Rockefeller University, New York, NY, USA, 1988.
2. Rigol, M.; Dunjko, V.; Olshanii, M. Thermalization and its mechanism for generic isolated quantum systems. *Nature* **2008**, *452*, 854–858. [CrossRef]
3. Santos, L.F.; Rigol, M. Onset of quantum chaos in one-dimensional bosonic and fermionic systems and its relation to thermalization. *Phys. Rev. E* **2010**, *81*, 036206. [CrossRef]
4. Popescu, S.; Short, A.J.; Winter, A. Entanglement and the foundations of statistical mechanics. *Nat. Phys.* **2006**, *2*, 754–758. [CrossRef]
5. Srednicki, M. Chaos and quantum thermalization. *Phys. Rev. E* **1994**, *50*, 888–901. [CrossRef] [PubMed]
6. Reimann, P. Typicality for Generalized Microcanonical Ensembles. *Phys. Rev. Lett.* **2007**, *99*, 160404. [CrossRef]
7. Eisert, J.; Friesdorf, M.; Gogolin, C. Quantum many-body systems out of equilibrium. *Nat. Phys.* **2015**, *11*, 124–130. [CrossRef]
8. Polkovnikov, A.; Sengupta, K.; Silva, A.; Vengalattore, M. Colloquium: Nonequilibrium dynamics of closed interacting quantum systems. *Rev. Mod. Phys.* **2011**, *83*, 863–883. [CrossRef]
9. Garcia-March, M.A.; van Frank, S.; Bonneau, M.; Schmiedmayer, J.; Lewenstein, M.; Santos, L.F. Relaxation, chaos, and thermalization in a three-mode model of a Bose–Einstein condensate. *New J. Phys.* **2018**, *20*, 113039. [CrossRef]

10. Tasaki, H. Typicality of Thermal Equilibrium and Thermalization in Isolated Macroscopic Quantum Systems. *J. Stat. Phys.* **2016**, *163*, 937–997. [CrossRef]
11. Reimann, P. Generalization of von Neumann's Approach to Thermalization. *Phys. Rev. Lett.* **2015**, *115*, 010403. [CrossRef] [PubMed]
12. Hosur, P.; Qi, X.L.; Roberts, D.A.; Yoshida, B. Chaos in quantum channels. *J. High Energy Phys.* **2016**, *2016*, 4. [CrossRef]
13. Ding, D.; Hayden, P.; Walter, M. Conditional mutual information of bipartite unitaries and scrambling. *J. High Energy Phys.* **2016**, *2016*, 145. [CrossRef]
14. Brown, W.G.; Fawzi, O. Scrambling speed of random quantum circuits. *arXiv* **2013**, arXiv:quant-ph/1210.6644.
15. Liu, Z.W.; Lloyd, S.; Zhu, E.; Zhu, H. Entanglement, quantum randomness, and complexity beyond scrambling. *J. High Energy Phys.* **2018**, *2018*, 41. [CrossRef]
16. Liu, Z.W.; Lloyd, S.; Zhu, E.Y.; Zhu, H. Generalized Entanglement Entropies of Quantum Designs. *Phys. Rev. Lett.* **2018**, *120*, 130502. [CrossRef]
17. Styliaris, G.; Anand, N.; Zanardi, P. Information Scrambling over Bipartitions: Equilibration, Entropy Production, and Typicality. *arXiv* **2020**, arXiv:quant-ph/2007.08570.
18. Hayden, P.; Preskill, J. Black holes as mirrors: Quantum information in random subsystems. *J. High Energy Phys.* **2007**, *2007*, 120. [CrossRef]
19. Shenker, S.H.; Stanford, D. Stringy effects in scrambling. *J. High Energy Phys.* **2015**, *2015*, 132. [CrossRef]
20. Kitaev, A. Hidden Correlations in the Hawking Radiation and Thermal Noise. Talk Given at the Fundamental Physics Prize Symposium, 2014. Available online: https://online.kitp.ucsb.edu/online/joint98/kitaev/ (accessed on 15 August 2021).
21. Cotler, J.S.; Gur-Ari, G.; Hanada, M.; Polchinski, J.; Saad, P.; Shenker, S.H.; Stanford, D.; Streicher, A.; Tezuka, M. Black holes and random matrices. *J. High Energy Phys.* **2017**, *2017*, 118. [CrossRef]
22. Yang, Z.C.; Hamma, A.; Giampaolo, S.M.; Mucciolo, E.R.; Chamon, C. Entanglement complexity in quantum many-body dynamics, thermalization, and localization. *Phys. Rev. B* **2017**, *96*, 020408. [CrossRef]
23. Chamon, C.; Hamma, A.; Mucciolo, E.R. Emergent Irreversibility and Entanglement Spectrum Statistics. *Phys. Rev. Lett.* **2014**, *112*, 240501. [CrossRef]
24. Harrow, A.W.; Low, R.A. Random Quantum Circuits are Approximate 2-designs. *Commun. Math. Phys.* **2009**, *291*, 257–302. [CrossRef]
25. Gharibyan, H.; Hanada, M.; Shenker, S.H.; Tezuka, M. Onset of random matrix behavior in scrambling systems. *J. High Energy Phys.* **2018**, *2018*, 124. [CrossRef]
26. Brown, W.G. Random Quantum Dynamics: From Random Quantum Circuits to Quantum Chaos. Ph.D. Thesis, Dartmouth College, Hanover, NH, USA, 2010.
27. Brown, W.G.; Viola, L. Convergence Rates for Arbitrary Statistical Moments of Random Quantum Circuits. *Phys. Rev. Lett.* **2010**, *104*, 250501. [CrossRef] [PubMed]
28. Nahum, A.; Vijay, S.; Haah, J. Operator Spreading in Random Unitary Circuits. *Phys. Rev. X* **2018**, *8*, 021014. [CrossRef]
29. Brown, A.R.; Susskind, L. Second law of quantum complexity. *Phys. Rev. D* **2018**, *97*, 086015. [CrossRef]
30. Dowling, M.R.; Nielsen, M.A. The geometry of quantum computation. *Quantum Inf. Comput.* **2008**, *8*, 861–899.
31. Zhou, T.; Luitz, D.J. Operator entanglement entropy of the time evolution operator in chaotic systems. *Phys. Rev. B* **2017**, *95*, 094206. [CrossRef]
32. Benenti, G.; Casati, G. How complex is quantum motion? *Phys. Rev. E* **2009**, *79*, 025201. [CrossRef]
33. Maldacena, J.; Shenker, S.H.; Stanford, D. A bound on chaos. *J. High Energy Phys.* **2016**, *2016*, 106. [CrossRef]
34. Lashkari, N.; Stanford, D.; Hastings, M.; Osborne, T.; Hayden, P. Towards the fast scrambling conjecture. *J. High Energy Phys.* **2013**, *2013*, 22. [CrossRef]
35. Xu, S.; Swingle, B. Locality, Quantum Fluctuations, and Scrambling. *Phys. Rev. X* **2019**, *9*, 031048. [CrossRef]
36. Anand, N.; Styliaris, G.; Kumari, M.; Zanardi, P. Quantum coherence as a signature of chaos. *arXiv* **2020**, arXiv:quant-ph/2009.02760.
37. Larkin, A.I.; Ovchinnikov, Y.N. Quasiclassical method in the theory of superconductivity. *J. Exp. Theor. Phys.* **1969**, *28*, 1200–1205.
38. Lin, C.J.; Motrunich, O.I. Out-of-time-ordered correlators in a quantum Ising chain. *Phys. Rev. B* **2018**, *97*, 144304. [CrossRef]
39. Chenu, A.; Molina-Vilaplana, J.; del Campo, A. Work Statistics, Loschmidt Echo and Information Scrambling in Chaotic Quantum Systems. *Quantum* **2019**, *3*, 127. [CrossRef]
40. Touil, A.; Deffner, S. Quantum scrambling and the growth of mutual information. *Quantum Sci. Technol.* **2020**, *5*, 035005. [CrossRef]
41. Häppölä, J.; Halász, G.B.; Hamma, A. Universality and robustness of revivals in the transverse field XY model. *Phys. Rev. A* **2012**, *85*, 032114. [CrossRef]
42. Swingle, B.; Bentsen, G.; Schleier-Smith, M.; Hayden, P. Measuring the scrambling of quantum information. *Phys. Rev. A* **2016**, *94*, 040302. [CrossRef]
43. von Keyserlingk, C.W.; Rakovszky, T.; Pollmann, F.; Sondhi, S.L. Operator Hydrodynamics, OTOCs, and Entanglement Growth in Systems without Conservation Laws. *Phys. Rev. X* **2018**, *8*, 021013. [CrossRef]
44. Swingle, B. Unscrambling the physics of out-of-time-order correlators. *Nat. Phys.* **2018**, *14*, 988–990. [CrossRef]

45. Huang, Y.; Brandão, F.G.S.L.; Zhang, Y.L. Finite-Size Scaling of Out-of-Time-Ordered Correlators at Late Times. *Phys. Rev. Lett.* **2019**, *123*, 010601. [CrossRef] [PubMed]
46. Scott, A.J. Optimizing quantum process tomography with unitary 2-designs. *J. Phys. A Math. Theor.* **2008**, *41*, 055308. [CrossRef]
47. Roberts, D.A.; Yoshida, B. Chaos and complexity by design. *J. High Energy Phys.* **2017**, *2017*, 121. [CrossRef]
48. Wigner, E.P. On the statistical distribution of the widths and spacings of nuclear resonance levels. *Math. Proc. Camb. Philos. Soc.* **1951**, *47*, 790–798. [CrossRef]
49. Haake, F.; Gnutzmann, S.; Kuś, M. *Quantum Signatures of Chaos*; Springer International Publishing: Berlin/Heidelberg, Germany, 2018. [CrossRef]
50. Mehta, M.L. *Random Matrices*; Elsevier: Amsterdam, The Netherlands, 1991. [CrossRef]
51. Tao, T. *Topics in Random Matrix Theory*; American Mathematical Society: Providence, RI, USA, 2012. [CrossRef]
52. Rao, W.J. Higher-order level spacings in random matrix theory based on Wigner's conjecture. *Phys. Rev. B* **2020**, *102*, 054202. [CrossRef]
53. Chen, X.; Zhou, T. Operator scrambling and quantum chaos. *arXiv* **2018**, arXiv:cond-mat.str-el/1804.08655.
54. Cotler, J.; Hunter-Jones, N.; Liu, J.; Yoshida, B. Chaos, complexity, and random matrices. *J. High Energy Phys.* **2017**, *2017*, 48. [CrossRef]
55. Hunter-Jones, N.R. Chaos and Randomness in Strongly-Interacting Quantum Systems. Ph.D. Thesis, California Institute of Technology, Pasadena, CA, USA, 2018.
56. Balasubramanian, V.; Berkooz, M.; Ross, S.F.; Simón, J. Black holes, entanglement and random matrices. *Class. Quantum Gravity* **2014**, *31*, 185009. [CrossRef]
57. Bao, J.H.; Zhang, C.Y. Out-of-time-order correlators in the one-dimensional XY model. *Commun. Theor. Phys.* **2020**, *72*, 085103. [CrossRef]
58. Scaramazza, J.A.; Shastry, B.S.; Yuzbashyan, E.A. Integrable matrix theory: Level statistics. *Phys. Rev. E* **2016**, *94*, 032106. [CrossRef] [PubMed]
59. Riser, R.; Kanzieper, E. Power spectrum and form factor in random diagonal matrices and integrable billiards. *arXiv* **2020**, arXiv:nlin.CD/2011.02210.
60. Prakash, A.; Pixley, J.H.; Kulkarni, M. The universal spectral form factor for many-body localization. *arXiv* **2020**, arXiv:cond-mat.dis-nn/2008.07547.
61. Riser, R.; Osipov, V.A.; Kanzieper, E. Nonperturbative theory of power spectrum in complex systems. *Ann. Phys.* **2020**, *413*, 168065. [CrossRef]
62. Brandão, F.G.S.L.; Ćwikliński, P.; Horodecki, M.; Horodecki, P.; Korbicz, J.K.; Mozrzymas, M. Convergence to equilibrium under a random Hamiltonian. *Phys. Rev. E* **2012**, *86*, 031101. [CrossRef]
63. Caravelli, F.; Coulter-De Wit, G.; García-Pintos, L.P.; Hamma, A. Random quantum batteries. *Phys. Rev. Res.* **2020**, *2*, 023095. [CrossRef]
64. Collins, B. Moments and cumulants of polynomial random variables on unitary groups, the Itzykson-Zuber integral, and free probability. *Int. Math. Res. Not.* **2003**, *2003*, 953–982. [CrossRef]
65. Roth, I.; Kueng, R.; Kimmel, S.; Liu, Y.K.; Gross, D.; Eisert, J.; Kliesch, M. Recovering Quantum Gates from Few Average Gate Fidelities. *Phys. Rev. Lett.* **2018**, *121*, 170502. [CrossRef]
66. Leone, L.; Oliviero, S.F.E.; Zhou, Y.; Hamma, A. Quantum Chaos is Quantum. *Quantum* **2021**, *5*, 453. [CrossRef]
67. Oliviero, S.F.E.; Leone, L.; Caravelli, F.; Hamma, A. Random Matrix Theory of the Isospectral twirling. *SciPost Phys.* **2021**, *10*, 76. [CrossRef]
68. Gemmer, J.; Michel, M.; Mahler, G. *Quantum Thermodynamics*; Springer: Berlin/Heidelberg, Germany, 2009. [CrossRef]
69. Canali, C.M.; Kravtsov, V.E. Normalization sum rule and spontaneous breaking of U(N) invariance in random matrix ensembles. *Phys. Rev. E* **1995**, *51*, R5185–R5188. [CrossRef]
70. Pato, M.P. Spontaneous symmetry breaking in $U(N)$ invariant ensembles with a soft confinement potential. *Phys. Rev. E* **2000**, *61*, R3291–R3294. [CrossRef]
71. Liu, J. Spectral form factors and late time quantum chaos. *Phys. Rev. D* **2018**, *98*, 086026. [CrossRef]
72. Yan, B.; Cincio, L.; Zurek, W.H. Information Scrambling and Loschmidt Echo. *Phys. Rev. Lett.* **2020**, *124*, 160603. [CrossRef]
73. Bhattacharyya, A.; Chemissany, W.; Haque, S.S.; Yan, B. Towards the Web of Quantum Chaos Diagnostics. *arXiv* **2019**, arXiv:hep-th/1909.01894.
74. Peres, A. Stability of quantum motion in chaotic and regular systems. *Phys. Rev. A* **1984**, *30*, 1610–1615. [CrossRef]
75. Weinstein, Y.S.; Lloyd, S.; Tsallis, C. Border between Regular and Chaotic Quantum Dynamics. *Phys. Rev. Lett.* **2002**, *89*, 214101. [CrossRef] [PubMed]
76. Kowalewska-Kudłaszyk, A.; Kalaga, J.; Leoński, W. Long-time fidelity and chaos for a kicked nonlinear oscillator system. *Phys. Lett. A* **2009**, *373*, 1334–1340. [CrossRef]
77. Choi, M. Completely positive linear maps on complex matrices. *Linear Algebra Its Appl.* **1975**, *10*, 285–290. [CrossRef]
78. Zanardi, P. Entanglement of quantum evolutions. *Phys. Rev. A* **2001**, *63*, 040304. [CrossRef]
79. Zhou, S.; Yang, Z.C.; Hamma, A.; Chamon, C. Single T gate in a Clifford circuit drives transition to universal entanglement spectrum statistics. *SciPost Phys.* **2020**, *9*, 87. [CrossRef]
80. Watrous, J. *The Theory of Quantum Information*; Cambridge University Press: Cambridge, UK, 2018. [CrossRef]